

Article

Generalized Interface Shear Strength Equation for Recycled Materials Reinforced with Geogrids

Artit Udomchai ¹, Menglim Hoy ^{1,2,3,*} , Apichat Suddeepong ^{2,3}, Amornrit Phuangsombat ⁴,
Suksun Horpibulsuk ^{1,2,3,5,*} , Arul Arulrajah ⁶ and Nguyen Chi Thanh ⁷

- ¹ School of Civil Engineering, Suranaree University of Technology, Nakhon Ratchasima 30000, Thailand; artit.u@g.sut.ac.th
 - ² School of Civil and Infrastructure Engineering, Suranaree University of Technology, Nakhon Ratchasima 30000, Thailand; suddeepong@g.sut.ac.th
 - ³ Center of Excellence in Innovation for Sustainable Infrastructure Development, Suranaree University of Technology, Nakhon Ratchasima 30000, Thailand
 - ⁴ Graduate Program in Construction and Infrastructure Management, Suranaree University of Technology, Nakhon Ratchasima 30000, Thailand; chaninnun@outlook.co.th
 - ⁵ Academy of Science, and Royal Society of Thailand, Bangkok 10300, Thailand
 - ⁶ Department of Civil and Construction Engineering, Swinburne University of Technology, Melbourne, VIC 3122, Australia; aarulrajah@swin.edu.au
 - ⁷ Department of Materials Technology, Faculty of Applied Sciences, Ho Chi Minh City University of Technology and Education, Ho Chi Minh City 70000, Vietnam; thanhnc@hcmute.edu.vn
- * Correspondence: menglim@g.sut.ac.th (M.H.); suksun@g.sut.ac.th (S.H.)



Citation: Udomchai, A.; Hoy, M.; Suddeepong, A.; Phuangsombat, A.; Horpibulsuk, S.; Arulrajah, A.; Thanh, N.C. Generalized Interface Shear Strength Equation for Recycled Materials Reinforced with Geogrids. *Sustainability* **2021**, *13*, 9446. <https://doi.org/10.3390/su13169446>

Academic Editor: Castorina Silva Vieira

Received: 14 July 2021

Accepted: 18 August 2021

Published: 23 August 2021

Publisher's Note: MDPI stays neutral with regard to jurisdictional claims in published maps and institutional affiliations.



Copyright: © 2021 by the authors. Licensee MDPI, Basel, Switzerland. This article is an open access article distributed under the terms and conditions of the Creative Commons Attribution (CC BY) license (<https://creativecommons.org/licenses/by/4.0/>).

Abstract: In this research, large direct shear tests were conducted to evaluate the interface shear strength between reclaimed asphalt pavement (RAP) and kenaf geogrid (RAP–geogrid) and to also assess their viability as an environmentally friendly base course material. The influence of factors such as the gradation of RAP particles and aperture sizes of geogrid (D) on interface shear strength of the RAP–geogrid interface was evaluated under different normal stresses. A critical analysis was conducted on the present and previous test data on geogrids reinforced recycled materials. The D/F_D , in which F_D is the recycled materials' particle content finer than the aperture of geogrid, was proposed as a prime parameter governing the interface shear strength. A generalized equation was proposed for predicting the interface shear strength of the form: $\alpha = a(D/F_D) + b$, where α is the interface shear strength coefficient, which is the ratio of the interface shear strength to the shear strength of recycled material, and a and b are constants. The constant values of a and b were found to be dependent upon types of recycled material, irrespective of types of geogrids. A stepwise procedure to determine variable a , which is required for analysis and design of geogrids reinforced recycled materials in roads with various gradations was also suggested.

Keywords: ground improvement; geogrid; recycled materials; interface shear strength; large-direct shear test; base course reinforcement; pavement geotechnics

1. Introduction

Roadways and highways are commonly categorized based on the traffic volumes and service life into two main categories—namely, permanent roads and temporary roads. Permanent roads are subjected to heavy traffic volumes of more than a million traffic loads during their service life. Temporary roads, on the other hand, are subject to lower traffic volumes of less than 10,000 load applications during their service life. Temporary roads include access roads, haul, detours, and construction platforms, which are used to construct permanent roads on weak soil layers [1].

Due to the scarcity of high-quality natural materials, marginal soils have been used for road construction with some form of mechanical or chemical treatment. Chemical

stabilization such as with cement, natural rubber latex stabilization [2–4], and geopolymer stabilization [5–7] are often used to enhance the mechanical properties of marginal materials.

Geogrid applications have also been found to improve the mechanical properties and performance of marginal materials for base/subbase courses [8–11]. Research on geosynthetics in pavement reinforcement application has reported that the use of a geogrid within an unbound layer of a pavement structure can improve the stiffness of pavement layers, especially below and above the location of the geogrid [1,12,13]. Geogrids stabilize the aggregate layer by increasing aggregate interlocking, enhancing confinement, and reducing the lateral movement of the pavement structure, leading to deformation reduction.

The advantages of utilizing geogrids in road construction include a decrease in the thickness of the pavement structure layers and prolonging the durability of the road structure. Geosynthetics reinforcement in asphalt layers has also been reported to reduce rutting, pavement material fatigue, as well as thermal and reflective cracking. Geocomposite materials, such as geotextiles sandwiched within geogrids are also used as a separation layer to prevent the movement of small particles into open-graded base layers, resulting in improving the drainage systems and enhancing the road performance [14].

In temporary roads, geogrids are used within the weak foundation to support the initial construction work. The geogrid-reinforced aggregates are used as a working platform to mobilize the heavy machinery into the construction sites. For a particular subgrade stabilization application, geogrids are used to reinforce the soft subgrade and to decrease the excessive deformation of pavement structures due to the traffic loads [15–18]. For basal reinforcement applications, geogrids are installed under or within unbound layers of a flexible road to enhance the bearing capacity of the pavement against cyclic loads [19,20]. For pavement surface reinforcement, geogrids are used within the asphalt layer to decrease fatigue and rutting of the pavement surface using the marginal quantity aggregate [21,22].

Annually across the globe, the construction industry generates large quantities of construction and demolition (C&D) wastes, including recycled concrete aggregate (RCA), as well as recycled glass and brick. Similarly, reclaimed asphalt pavement (RAP) is generated when asphalt pavements are removed for reconstruction and/or resurfacing. Road authorities in many countries have been seeking to develop innovative methods of recycling and reusing recycled aggregates for partial or total replacement of natural aggregates in road-work applications. The use of recycled aggregates including RAP [23–25], RCA [26–28], and recycled glass [29–31] as an alternative aggregate is widely accepted for road construction, especially as pavement base/subbase materials. Reusing recycled materials can decrease waste and energy consumption and therefore significantly contributes toward the sustainable road construction industry [32,33]. However, these materials sometimes require mechanical improvement to meet the local and international standards for both design and construction.

Several researchers have reported on the successful application of commercial synthetic geogrids reinforced natural materials in road construction. However, the applications of geogrid-reinforced recycled aggregates remain limited due to the lack of research studies, accepted design methodology, and construction guidelines. Pioneering research on the commercial geogrid-reinforced recycled aggregates was recently undertaken by several researchers [29,34–39]. Suddepong et al. (2021) [40] investigated the interface shear behavior of natural kenaf geotextiles and RCA to promote the use of natural geotextiles with recycled aggregates for sustainable development of road construction and environmentally sound technologies. The performance of geogrid-reinforced recycled aggregates relies on various factors such as geometric forms and stiffness of geogrid, location and depth of geogrid installation, and particle sizes of aggregates [34,35,40].

This research aims to further contribute to the increased utilization of recycled aggregates in the pavement structure and to also facilitate the analysis and design by developing a generalized predictive equation of interface shear strength between geogrid and recycled aggregates. A large direct shear test (LDST) was first conducted to determine the interface shear strength behavior of RAP reinforced with natural kenaf geogrid in this research.

The influence of gradation of RAP and aperture size of geogrid on the interface shear responses of RAP—geogrid under different normal stresses was investigated. The results were then compared with the previous results to introduce a prime factor for developing a generalized predictive equation that can be used for rapid estimation of the interface shear strength of recycled aggregates reinforced with both commercial and natural geogrids.

2. Materials and Methods

2.1. Materials

Reclaimed asphalt pavement (RAP) samples were obtained from the Bureau of Highways, Nakhon Ratchasima, Thailand. A cold milling machine was used to remove the asphalt pavement for resurfacing in the cold in-place recycling process. The asphalt content in RAP aggregate is approximately 3–5% by weight. Figure 1 indicates the gradations of large-sized RAP and small-sized RAP samples. The large-sized RAP is on the lower boundary and the small-sized RAP is on the upper boundary, designated by the Department of Highways, Thailand (DOH, 2001) [41].

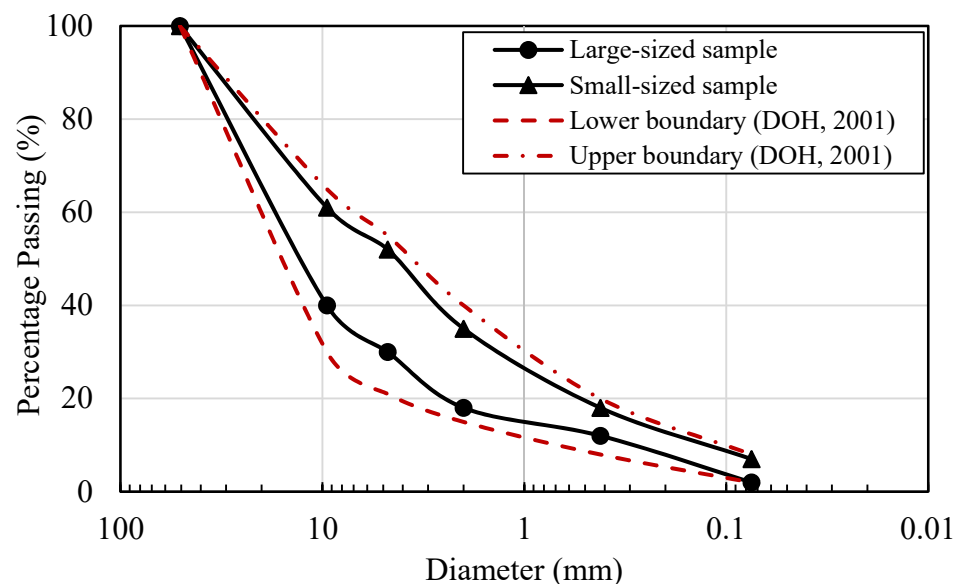


Figure 1. Grain size distribution of RAP.

Table 1 summarizes the basic and engineering properties of the RAP samples. The large-sized RAP and small-sized RAP samples were classified as poorly graded gravel (GP) and well-graded gravel (GW), respectively, according to the Unified Soil Classification System. Although the average particle size of the large-sized RAP sample and small-sized RAP sample was different, the specific gravity, maximum dry density (MDD) at optimum water content, California bearing ratio, internal friction angles, and cohesion were almost the same.

Table 1. Basic engineering properties of RAP samples.

Parameter	Recycled Asphalt Pavement (RAP)	
	Large Sized	Small Sized
Bulk specific gravity	2.6	2.6
Soil classification (USCS)	GP	GW
Average particle size (mm)	17	3.7
Optimum water content (%)	13.70	13.80
Maximum dry unit weight (kN/m^3)	19.56	19.48
California bearing ratio (%)	20	20
Internal friction angle (degree)	56.99	54.81
Cohesion (kPa)	53.68	56.98

The natural kenaf fibers were obtained from Tai Song Huad Co., Ltd., Sai Mai, Bangkok, Thailand, and were used to fabricate kenaf geogrid in this research. The handmade biaxial kenaf geogrid was a planar grid, which possesses the same strength in both ortho-directions (longitudinal and transversal) (Figure 2). The single rib tensile strength of kenaf geogrid was 43 MPa, which was obtained from the tensile test using a universal testing machine with a capacity of 2.5 kN based on ASTM-D6637 (2015) [42]. Two different aperture sizes of kenaf geogrids: 7×7 mm and 21×21 mm with a 3 mm rib thickness were prepared.

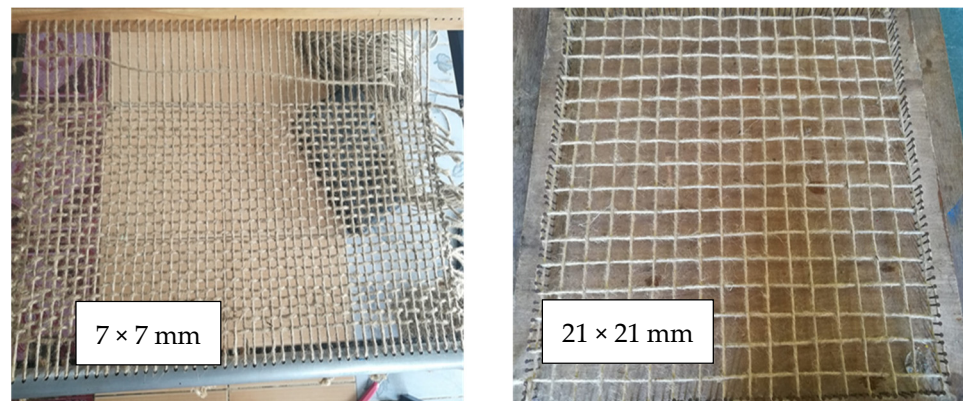


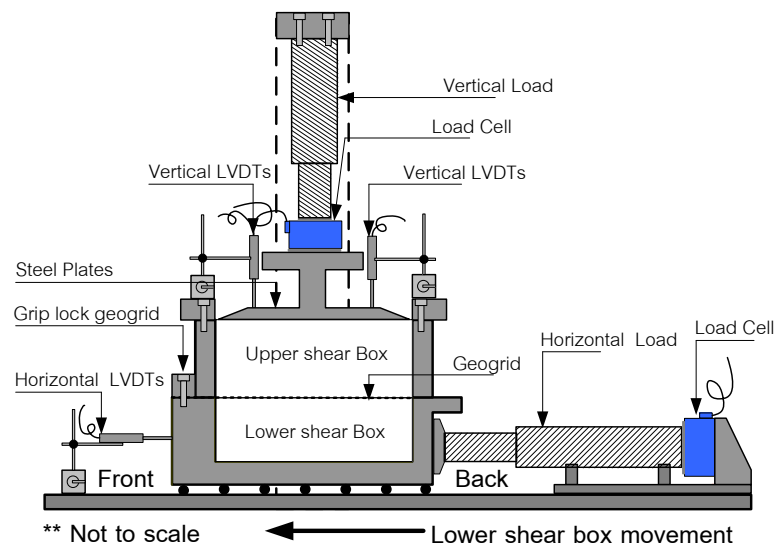
Figure 2. Photos of the planar grid of handmade biaxial kenaf geogrids.

2.2. Experimental Program

The LDST was undertaken in accordance with ASTM-D5321 (2020) [43] to investigate the interface shear strength of RAP–geogrid samples ($\tau_{\text{reinforced}}$) and the shear strength of unreinforced RAP samples ($\tau_{\text{unreinforced}}$). The LDST shear box apparatus with a dimension of 305×305 mm² and 204 mm high was divided into two parts, whereby the stationary upper half provides a confined vertical load to the sample, while the lower half of the box allows the application of horizontal shearing stress. To conduct the shear test, hand compaction was first carried out on RAP samples at optimum water content in three layers in the shear box under the modified Proctor effort to attain the MDD. For the consolidation process, the lower shear box and half of the upper one were filled with de-aired water to saturate the compacted RAP samples under different normal stresses ($\sigma_n = 50, 100,$ and 200 kPa) for 12 h. LDSTs were conducted at the same σ_n levels with a constant shear rate of 0.025 mm/min at a controlled temperature of 20 ± 1 °C. The tests were completed when the horizontal shear displacement (HSD) attained 40 mm. Three samples were carried out for each direct shear test, and the mean value was reported in this study. The results under the same testing condition were reproducible with a low mean standard deviation, SD ($SD/\bar{x} < 10\%$, where \bar{x} is the mean value). Table 2 illustrates the names of the prepared sample for LDST. Figure 3 illustrates the LDST apparatus and a photo of the tested kenaf geogrid.

Table 2. Summary of LDST testing program.

RAP Sample	Reinforcement	Normal Stress (kPa)
Large size	No reinforcement	50, 100, 200
	RAP + 7×7 mm geogrid	50, 100, 200
	RAP + 21×21 mm geogrid	50, 100, 200
Small size	No reinforcement	50, 100, 200
	RAP + 7×7 mm geogrid	50, 100, 200
	RAP + 21×21 mm geogrid	50, 100, 200



(a)



(b)

Figure 3. (a) LDST apparatus and (b) a photo of the tested kenaf geogrid.

3. Results and Discussion

The shear stresses and dilatation characteristics of unreinforced RAP obtained from the LDST were demonstrated in Figure 4. The shear stress behaviors of large-sized RAP and small-sized RAP were similar. The shear strength of unreinforced material ($\tau_{\text{unreinforced}}$) versus horizontal shear displacement (HSD) relationship exhibited strain-hardening behavior, whereby the shear stress increased with horizontal displacement and then became almost constant after HSD = 20-mm. The maximum $\tau_{\text{unreinforced}}$ increased with the increased σ_n .

The vertical shear displacement (VSD) versus HSD relationship of both large-sized RAP and small-sized RAP exhibited dilative behavior, which behaved similar to dense recycled glass [44] and RCA [35], at high σ_n of 100–200 kPa. The VSD of large- and small-sized RAP samples were similar when the HSD < 20 mm. However, the VSD of the small-sized RAP was higher than that of the large-sized RAP when the HSD was > 20 mm, especially at a high $\sigma_n = 200$ kPa.

In accordance with the Mohr–Coulomb failure criterion, the friction angle (ϕ) and cohesion (c) at the peak for both large-sized RAP and small-sized RAP samples were determined and are illustrated in Figure 5. The ϕ and c of small-sized RAP samples ($\phi = 54.81^\circ$ and $c = 56.99$ kPa) and large-sized RAP samples ($\phi = 56.99^\circ$ and $c = 53.68$ kPa) were similar. The high shear strength properties of RAP samples demonstrate that the material is stiff to withstand the traffic load and can be used as a base/subbase material based on the Department of Highways (DOH) specification [41]. The results also indicated

that the RAP samples with gradation within the boundary specified by DOH can be used as base/subbase materials.

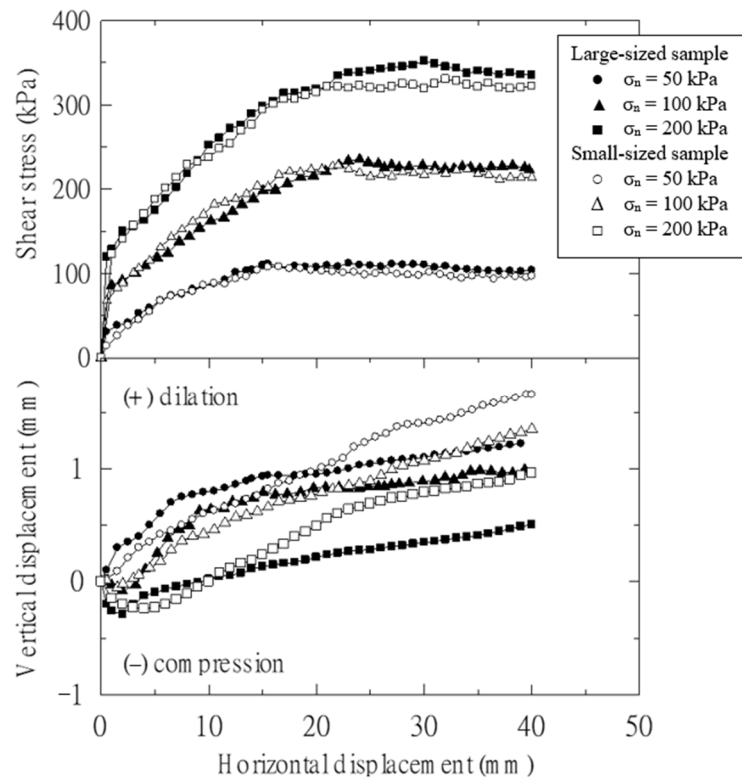


Figure 4. LDST test results of unreinforced RAP.

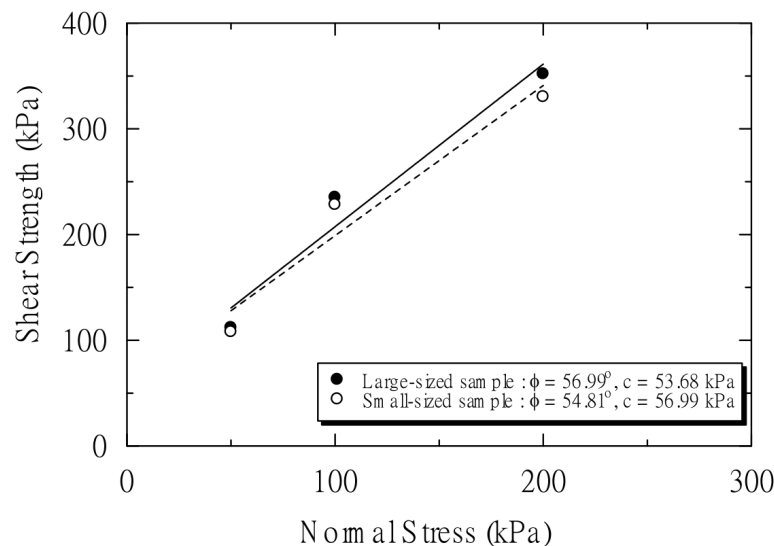


Figure 5. Shear strength failure envelope for unreinforced RAP.

Figures 6 and 7, respectively, indicate the influence of aperture sizes of kenaf geogrid (D) on the $\tau_{\text{reinforced}}$ behaviors of large-sized RAP–geogrid and small-sized RAP–geogrid. The $\tau_{\text{reinforced}}$ behavior of large-sized RAP samples was similar to that of the small-sized ones. $\tau_{\text{reinforced}}$, stiffness, and its peak values were found to increase with the increase in σ_n from 50 to 200 kPa. The relationship between $\tau_{\text{reinforced}}$ versus HSD of RAP–geogrid samples for both RAP gradations indicated strain-hardening behavior, similar to unreinforced RAP samples.

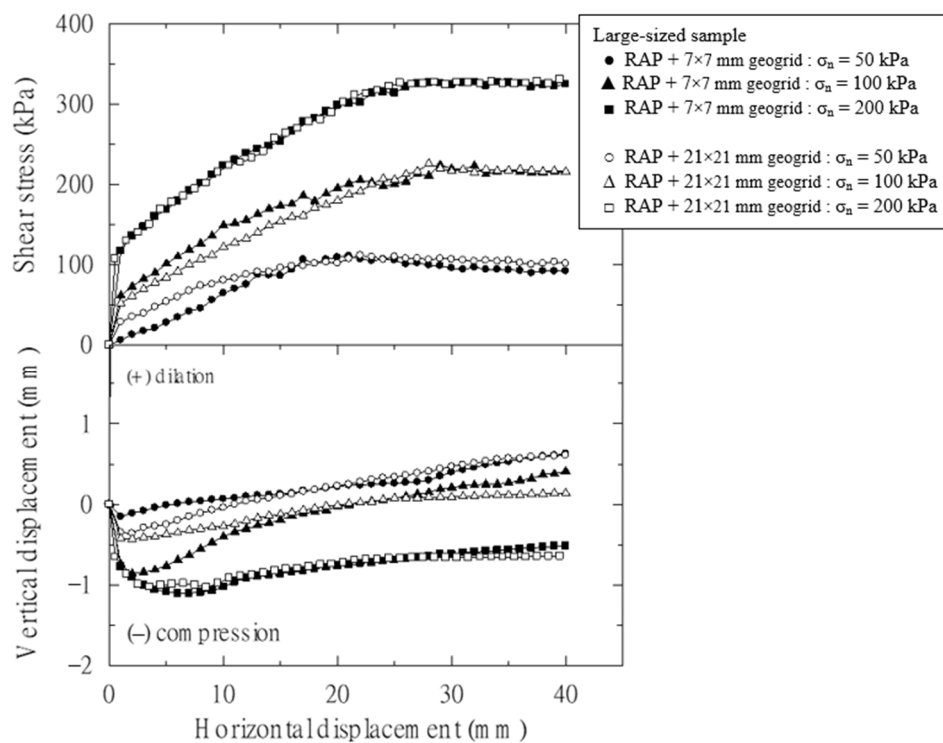


Figure 6. Effect of aperture size of geogrid on shear interface between geogrid and large-sized RAP sample.

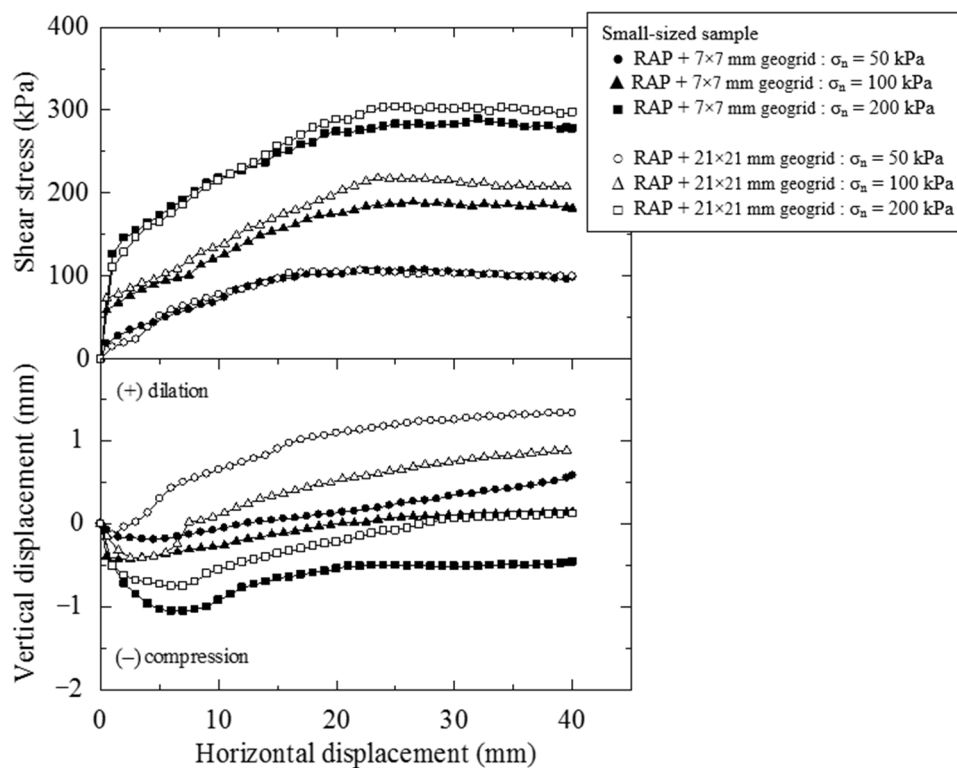


Figure 7. Effect of aperture size of geogrid on shear interface between geogrid and small-sized RAP sample.

For the large-sized RAP samples (Figure 6), the peak $\tau_{\text{reinforced}}$ of the samples at $\sigma_n = 50$ kPa was found at an HSD of approximately 20 to 25 mm. The peak $\tau_{\text{reinforced}}$ of the samples at σ_n of 100–200 kPa was, however, found at a large HSD of approximately

30 to 40 mm. For the small-sized RAP samples, the peak $\tau_{\text{reinforced}}$ of the samples was at an HSD of approximately 25 to 35 mm for all σ_n (Figure 7). The peak $\tau_{\text{reinforced}}$ of kenaf geogrid-reinforced small-sized RAP samples was slightly lower than those of kenaf geogrid-reinforced large-sized RAP samples at the same σ_n .

The relationship between VSD and HSD of RAP–geogrid with large- and small-sized RAP samples is also shown in Figures 6 and 7, respectively. A contraction behavior is noticed at an early stage, followed by continuous dilative behavior at the final stage. The dilative vertical displacements of kenaf geogrid-reinforced both large- and small-sized RAP samples were higher than those of unreinforced RAP samples at the same σ_n . This implies that the interaction between geogrid and RAP particles was improved. The influence of kenaf geogrid aperture size on VSD versus HSD relation was clearly apparent for the small-sized RAP samples. At a particular σ_n , the VSD of kenaf geogrid-reinforced small-sized RAP samples with 7×7 mm geogrid was higher than that of samples with 21×21 mm geogrid at the same HSD. The $\tau_{\text{reinforced}}$ value of RAP–geogrid samples was dependent upon both RAP aggregate interlocking and the contact surface area between RAP particles and geogrid.

Figures 8 and 9 show the Mohr–Coulomb failure envelopes of RAP–geogrids with different aperture sizes of geogrid and different gradations of RAP samples, compared with the failure envelopes of unreinforced RAP samples. For the large-sized RAP sample (Figure 8), the friction angle of unreinforced RAP samples ($\phi = 56.99^\circ$) was slightly higher than the interface friction angles of kenaf geogrid-reinforced RAP samples with 21×21 mm geogrid ($\delta = 55.06^\circ$) and 7×7 mm ($\delta = 54.18^\circ$). In contrast, the adhesion values of kenaf geogrid-reinforced RAP samples with 21×21 mm geogrid ($c_a = 56.92$ kPa), 7×7 mm geogrid ($c_a = 59.29$ kPa) were higher than the cohesion of unreinforced RAP samples ($c = 53.68$ kPa). For small-sized RAP samples (Figure 9), the interface friction angles of kenaf geogrid-reinforced RAP samples were similar for both aperture sizes of 21×21 mm geogrid ($\delta = 51.26^\circ$) and 7×7 mm geogrid ($\delta = 50.34^\circ$). These values were lower than the friction angle of the unreinforced RAP samples ($\phi = 54.81^\circ$). The adhesion values of kenaf geogrid-reinforced RAP samples with 21×21 mm geogrid and 7×7 mm geogrid were 64.41 kPa and 53.12 kPa, respectively, while the cohesion value of the unreinforced RAP sample was 56.99 kPa. This reveals that the aperture size of geogrid and gradation of RAP particles had a significant influence on the $\tau_{\text{reinforced}}$ value of kenaf geogrid-reinforced RAP samples. The interface shear strength ($\tau_{\text{reinforced}}$) of RAP–geogrid samples was found to be lower than the $\tau_{\text{unreinforced}}$ of unreinforced RAP samples, which are consistent with the previous findings [29,35,40,45]. For all sizes of RAP samples, the higher aperture size of kenaf geogrid resulted in the higher adhesion but insignificantly affected the interface friction angles.

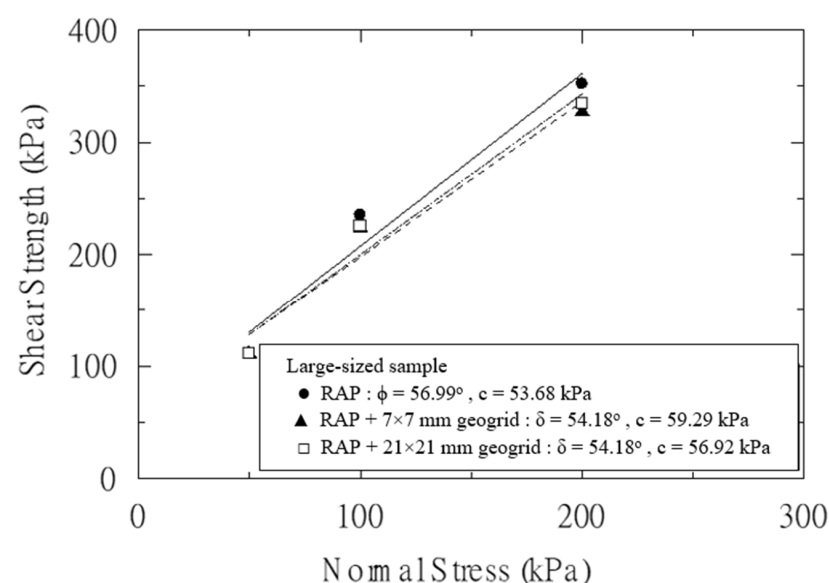


Figure 8. Interface stress failure envelopes for large-sized RAP samples.

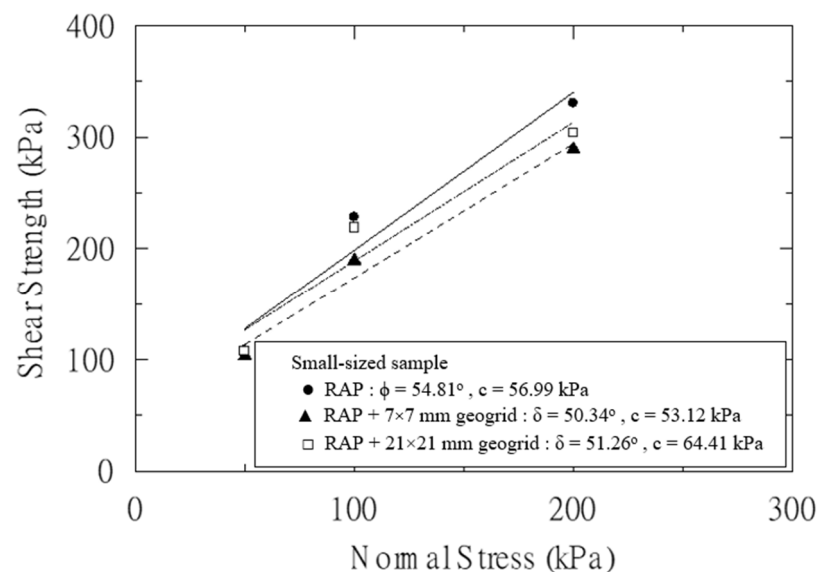


Figure 9. Interface stress failure envelopes for small-sized RAP samples.

To facilitate the analysis and design for pavement geotechnics applications, particularly by the finite element method, it is useful to interpret the $\tau_{\text{reinforced}}$ using the interface shear strength coefficient (α) in the following expression [46,47]:

$$\alpha = \frac{\tau_{\text{reinforced}}}{\tau_{\text{unreinforced}}} \quad (1)$$

The correlation between α and σ_n of RAP–geogrid samples for large- and small-sized RAP samples is presented in Figure 10. Though the $\tau_{\text{unreinforced}}$ value of unreinforced RAP directly influenced the $\tau_{\text{unreinforced}}$ value of RAP–geogrid samples, it was found that the α was irrespective of σ_n . The aperture size of geogrid (D) and gradation of RAP samples were found to strongly affect the interlocking mechanism of geogrid reinforcement and aggregates. The RAP particle content finer than the geogrid aperture size (F_D), which is related to the influence of gradation of RAP samples on the interface shear strength is investigated. In other words, F_D is the percentage passing obtained from the grain size distribution of RAP that is smaller than the aperture size of geogrid ($D = 7 \times 7$ mm and 21×21 mm). The relationship between α versus D and between α versus F_D is depicted in Figures 11 and 12, respectively.

The effect of F_D on the α values of RAP–geogrid samples with different D and gradations of RAP samples is depicted in Figure 12. The effect of F_D on the α values was found to be similar to the effect of D on α values (Figure 11). For the small-sized RAP samples, the large aperture size (21×21 mm) of geogrid exhibited higher α values than the small aperture size (7×7 mm), while the α values were found to be practically the same for both aperture sizes (21×21 mm and 7×7 mm) of geogrid-reinforced RAP samples, although F_D was varied from 0.28 to 0.6. However, for the same F_D of 0.6, the large-sized RAP + 21×21 mm geogrid had higher α than the small-sized RAP + 7×7 mm geogrid. It seems that $F_D = 0.28$ for large-sized RAP and $F_D = 0.8$ for small-sized RAP yielded the same α value of 0.96. In other words, both F_D and D control the α value.

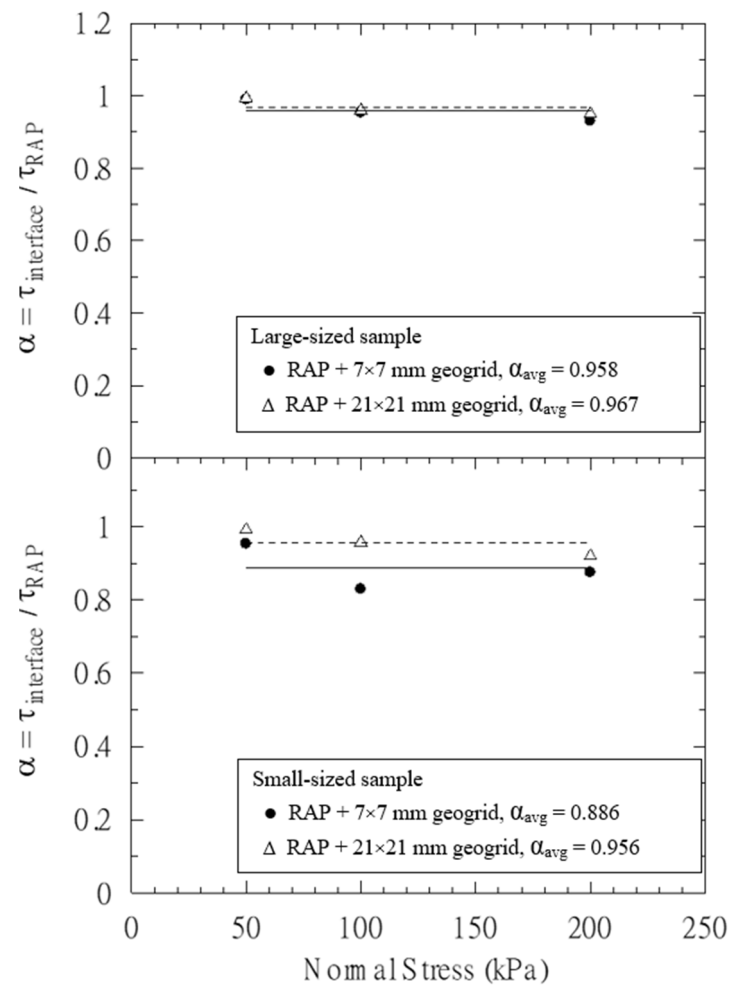


Figure 10. Relationship between α and normal stress.

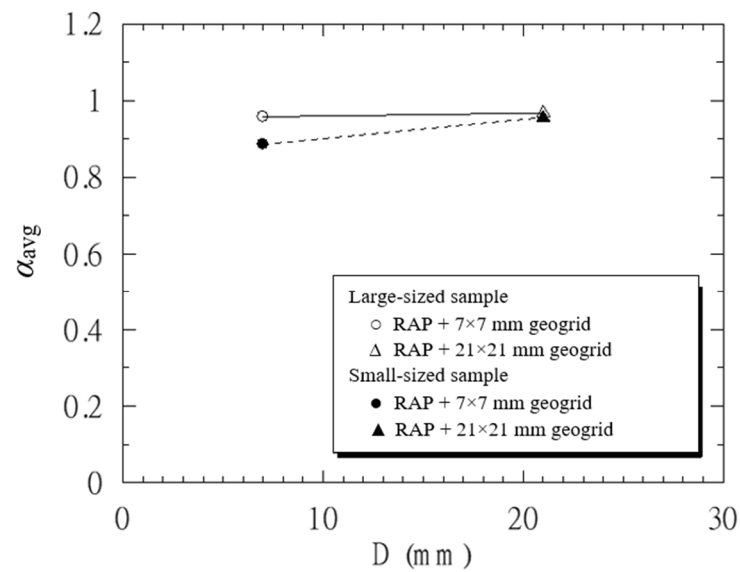


Figure 11. Effect of the aperture width of geogrid on the interface shear strength coefficient.

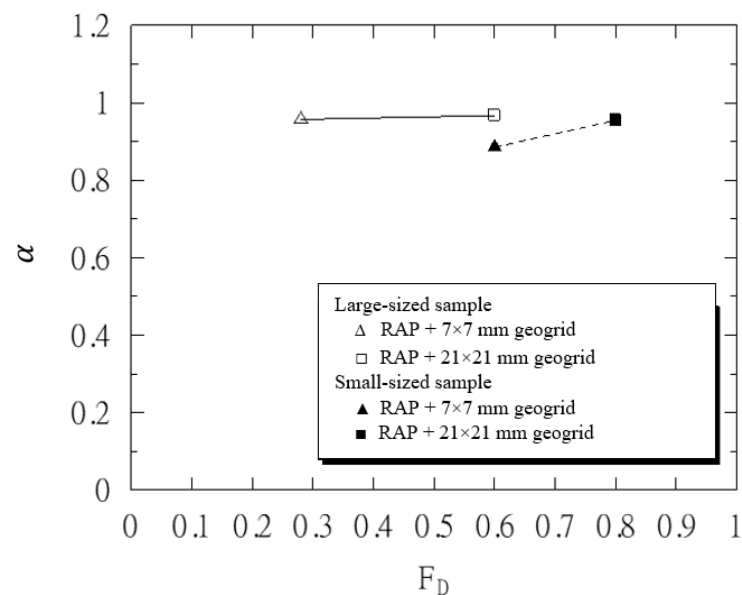


Figure 12. Effect of particle content finer than the aperture width of geogrid on the interface shear strength coefficient.

The relationship between α and D for the small-sized RAP samples (Figure 11) showed that the large aperture size (21×21 mm) of geogrid resulted in higher α values than the small aperture size (7×7 mm) of geogrid. In contrast, the α values of the large-sized RAP samples were found to be essentially the same for both large and small aperture sizes of geogrid. In addition, the α values of the large-sized RAP and small-sized RAP samples were similar for the 21×21 mm aperture size of geogrid, while the α value of small-sized RAP samples was lower than that of large-sized RAP samples with 7×7 mm geogrid. This implies that the aperture size of geogrid influences the α values of kenaf geogrid-reinforced RAP samples and ideally, a very large D results in the same α for different RAP gradations.

Several researchers have investigated the effect of a ratio of D to average aggregate particle size (D_{50}) on the $\tau_{\text{reinforced}}$ value of geogrid-reinforced aggregates [8,48,49]. However, the use of D_{50} to interpret the influence of the $\tau_{\text{reinforced}}$ behavior of geogrid-reinforced aggregate remains elusive. The proportion of aggregates indicated by D_{50} might have a large variation in large- and small-sized particles, which can significantly influence the gradation of the recycled materials. Consequently, excessively small or large particles of aggregates impact the effectiveness of the interlock mechanism or the $\tau_{\text{reinforced}}$ value of geogrid-reinforced recycled materials [50]. Some researchers studied the effect of a ratio of D to a single-sized gradation on the $\tau_{\text{reinforced}}$ behavior of geogrid-reinforced aggregates [51]. On the other hand, the use of a single-size particle or a poorly gradation of aggregate might not be suitable for pavement material in some road projects. Therefore, the use of the correlation between α versus D/F_D compliance for interpreting $\tau_{\text{reinforced}}$ of geogrid-reinforced recycled materials is a sound principle in this study.

Using the D/F_D as a prime parameter and integrating the contribution from D and F_D , the correlation between α and D/F_D is presented in Figure 13 and Equation (2) in the following expression:

$$\alpha = 0.0037 \left(\frac{D}{F_D} \right) + 0.85; 10 < \frac{D}{F_D} < 35 \text{ (mm)} \quad (2)$$

where D is expressed in mm, and F_D is expressed in decimal with a high degree of coefficient, determined as 0.94.

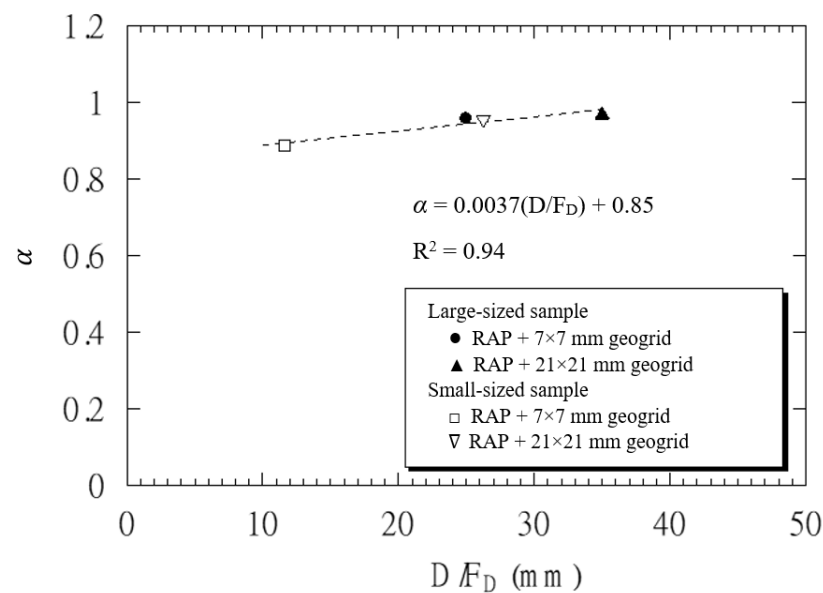


Figure 13. Relationship between α and D/F_D of kenaf geogrid-reinforced RAP samples.

Equation (2) is a useful practical tool for geotechnical and pavement engineers and the rational development of the equation can be extended to develop a generalized equation for different types of recycled materials and geogrids. Therefore, the separate set of data from the previous studies on the $\tau_{\text{reinforced}}$ behavior of the commercial polymer and natural kenaf geogrid-reinforced recycled aggregates such as RAP and RCA were taken and reanalyzed. Figure 14 shows the relationship between α and D/F_D of geogrid-reinforced RAP and RCA samples. The general form of the relationship can be expressed as the following equation:

$$\alpha = a \left(\frac{D}{F_D} \right) + b; 10 < \frac{D}{F_D} < 40 \text{ (mm)} \quad (3)$$

where a and b are constant. It is worthwhile mentioning that values of a and b are irrespective of geogrid types (natural kenaf or commercial polymer), while they were mainly dependent upon the recycled materials. From the regression analysis, the values of $a = 0.0046$ and $b = 0.8336$ were obtained for geogrid-reinforced RAP samples, while values of $a = 0.0057$ and $b = 0.7185$ were for geogrid-reinforced RCA samples. This implies that the geogrid-reinforced RAP has a higher α value than the geogrid-reinforced RCA at the same D/F_D for both natural kenaf and commercial polymer type. This might be due to the difference in shear strength, stiffness, and impurity of the recycled materials. The shear strength and stiffness of unreinforced RCA were higher than that of the unreinforced RAP material [34,51,52]. In other words, the geogrid-reinforced RCA samples exhibited a better interlocking mechanism than that geogrid-reinforced RAP samples. The α of RAP–geogrid is found to be more sensitive to the D/F_D than that of RAP–geogrid sample. Logically, there is no interaction between kenaf geogrid and RAP particles when $\tau_{\text{reinforced}}$ and $\tau_{\text{unreinforced}}$ are equal ($\alpha = 1.0$). Based on equation (3), the geogrid-reinforced RAP and geogrid-reinforced RCA have no interaction when $D = 36.2F_D$ and $D = 49.4F_D$, respectively.

The proposed equation was developed based on sound principles and can therefore be used to predict the α of the recycled materials reinforced with various geogrids once the values of the constants a and b are known. In practice, a stepwise procedure to determine α values for the design of geogrids stabilized base/subbase with recycled aggregates is proposed as follows:

- (1) From a selected recycled aggregate, adjust its gradation to meet the requirement for base/subbase courses specified by local or international standards;
- (2) From the gradation, which might be varied along the constructing road, select at least two gradations to determine D/F_D values for a selected geogrid;

- (3) Perform the direct shear test on the selected recycled aggregate at various normal stresses in the range of field working stress;
- (4) Perform the direct interface shear test on the recycled aggregate reinforced with geogrid at various normal stress and D/F_D values;
- (5) From Equation (3), determine values of a and b . With these two values, the α values of the selected geogrid and recycled aggregate can be approximated.

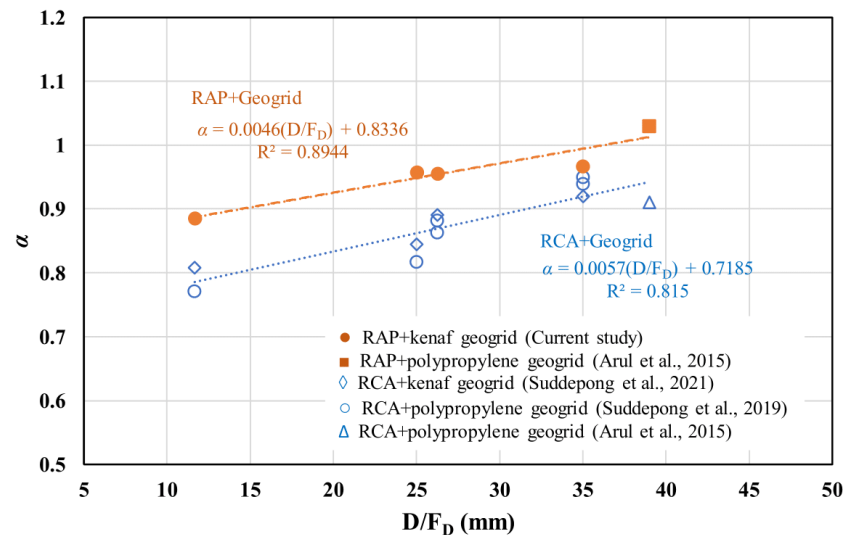


Figure 14. Relationship between α and D/F_D of geogrid-reinforced C&D samples.

This proposed general equation can be used to estimate the α for analysis and design of related geotechnical projects including pavement projects, mechanically stabilized earth (MSE) wall design, embankment reinforcement construction, and foundation design, which deal with various types of geogrid-reinforced recycled aggregates. Furthermore, to fully understand the behavior of natural geogrid-reinforced recycled aggregates, the relevant experimental program including dynamic flexural strength and fatigue tests are suggested for further research [53]. The outcome of this research will lead to the promotion of recycled aggregates as green aggregate for sustainable geotechnical and pavement applications.

4. Conclusions

In this research, a large direct shear test (LDST) was conducted to investigate the interface shear strength ($\tau_{\text{reinforced}}$) between reclaimed asphalt pavement (RAP) and kenaf geogrid (RAP-geogrid) as a sustainable base course material. The influence of gradation of RAP particles and aperture sizes of geogrid (D) on $\tau_{\text{reinforced}}$ of RAP-geogrid was evaluated under different normal stresses. Based on the critical analysis of the present and previous test data on both natural and commercial geogrid-reinforced C&D materials including RAP and RCA, it is found that the $\tau_{\text{reinforced}}$ value of geogrid-reinforced recycled materials was controlled by the D/F_D , where F_D is the recycled materials' particle content finer than the aperture of geogrid. The generalized equation for predicting $\tau_{\text{reinforced}}$ is proposed in the form: $\alpha = a(D/F_D) + b$, where α is interface shear strength coefficient, which is the ratio of $\tau_{\text{reinforced}}$ to $\tau_{\text{unreinforced}}$ of recycled material, and a and b are constant. The values of a and b were found to be dependent upon types of recycled material, irrespective of types of geogrids. This proposed generalized equation is useful to determine α , a required parameter for analysis and design of geotechnical and pavement work dealt with the geogrid-reinforced recycled aggregates. It is advantageous to the designer to select the various aperture sizes of geogrids and gradations of recycled aggregates for geotechnical and pavement projects.

Author Contributions: Conceptualization, A.U., A.S., M.H. and S.H.; methodology, A.U., M.H., A.P. and S.H.; software, A.U., A.P. and M.H.; formal analysis, A.U., A.S. and M.H.; writing—review and editing, A.U., A.S., S.H., M.H., N.C.T. and A.A.; visualization, M.H., A.A. and S.H.; supervision, M.H., A.A. and S.H. All authors have read and agreed to the published version of the manuscript.

Funding: Thailand Research Fund under Research and Researcher for Industries-RRI Program (Grant Number Phd62I0026).

Institutional Review Board Statement: Not applicable.

Informed Consent Statement: Not applicable.

Data Availability Statement: The data presented in this study are available on request from the corresponding author.

Acknowledgments: This work was financially supported by the Thailand Research Fund under Research and Researcher for Industries-RRI Program (Grant Number Phd62I0026).

Conflicts of Interest: The authors declare no conflict of interest.

References

- Holz, R.; Christopher, B.R.; Berg, R.R. *Geosynthetic Design and Construction Guidelines*; FHWA Publication No. FHWA HI-07-092; Federal Highway Administration: Washington, DC, USA, 1998.
- Buritatum, A.; Horpibulsuk, S.; Udomchai, A.; Suddeepong, A.; Takaikaew, T.; Vichitcholchai, N.; Arulrajah, A. Durability improvement of cement stabilized pavement base using natural rubber latex. *Transp. Geotech.* **2021**, 100518. [[CrossRef](#)]
- Buritatum, A.; Takaikaew, T.; Horpibulsuk, S.; Udomchai, A.; Hoy, M.; Vichitcholchai, N.; Arulrajah, A. Mechanical Strength Improvement of Cement-Stabilized Soil Using Natural Rubber Latex for Pavement Base Applications. *J. Mater. Civ. Eng.* **2020**, *32*, 04020372. [[CrossRef](#)]
- Jose, A.; Kasthurba, A. Laterite soil-cement blocks modified using natural rubber latex: Assessment of its properties and performance. *Constr. Build. Mater.* **2021**, *273*, 121991. [[CrossRef](#)]
- Avirneni, D.; Peddinti, P.R.; Saride, S. Durability and long term performance of geopolymer stabilized reclaimed asphalt pavement base courses. *Constr. Build. Mater.* **2016**, *121*, 198–209. [[CrossRef](#)]
- Phummiphon, I.; Horpibulsuk, S.; Rachan, R.; Arulrajah, A.; Shen, S.-L.; Chindaprasirt, P. High calcium fly ash geopolymer stabilized lateritic soil and granulated blast furnace slag blends as a pavement base material. *J. Hazard. Mater.* **2018**, *341*, 257–267. [[CrossRef](#)]
- Xiao, R.; Polaczyk, P.; Zhang, M.; Jiang, X.; Zhang, Y.; Huang, B.; Hu, W. Evaluation of glass powder-based geopolymer stabilized road bases containing recycled waste glass aggregate. *Transp. Res. Rec.* **2020**, *2674*, 22–32. [[CrossRef](#)]
- Giroud, J.P.; Han, J. Design Method for Geogrid-Reinforced Unpaved Roads. I. Development of Design Method. *J. Geotech. Geoenviron. Eng.* **2004**, *130*, 775–786. [[CrossRef](#)]
- Maghool, F.; Arulrajah, A.; Mirzababaei, M.; Suksiripattanapong, C.; Horpibulsuk, S. Interface shear strength properties of geogrid-reinforced steel slags using a large-scale direct shear testing apparatus. *Geotext. Geomembr.* **2020**, *48*, 625–633. [[CrossRef](#)]
- Saberian, M.; Li, J.; Perera, S.T.A.M.; Zhou, A.; Roychand, R.; Ren, G. Large-scale direct shear testing of waste crushed rock reinforced with waste rubber as pavement base/subbase materials. *Transp. Geotech.* **2021**, *28*, 100546. [[CrossRef](#)]
- Vieira, C.S. Valorization of Fine-Grain Construction and Demolition (C&D) Waste in Geosynthetic Reinforced Structures. *Waste Biomass Valorization* **2020**, *11*, 1615–1626.
- Christopher, B.; Perkins, S. Full scale testing of geogrids to evaluate junction strength requirements for reinforced roadway base design. In Proceedings of the Fourth European Geosynthetics Conference, Edinburgh, UK, 7–10 September 2008.
- Perkins, S.; Christopher, B.; Thom, N.; Montestruque, G.; Korkiala-Tanttu, L.; Want, A. Geosynthetics in pavement reinforcement applications. In Proceedings of the 9th International Conference on Geosynthetics, Guarujá, Brazil, 23–27 May 2010.
- Rajagopal, K.; Krishnaswamy, N.R.; Madhavi Latha, G. Behaviour of sand confined with single and multiple geocells. *Geotext. Geomembr.* **1999**, *17*, 171–184. [[CrossRef](#)]
- Al-Qadi, I.L.; Brandon, T.L.; Valentine, R.J.; Lacina, B.A.; Smith, T.E. Laboratory evaluation of geosynthetic-reinforced pavement sections. *Transp. Res. Rec.* **1994**, *1439*, 25–31.
- Cuelho, E.V.; Perkins, S.W. Geosynthetic subgrade stabilization—Field testing and design method calibration. *Transp. Geotech.* **2017**, *10*, 22–34. [[CrossRef](#)]
- Perkins, S.W. Numerical Modeling of Geosynthetic Reinforced Flexible Pavements. *Constr. Build. Mater.* **2016**, *122*, 214–230.
- Shirazi, M.G.; Rashid, A.S.A.; Nazir, R.; Abdul Rashid, A.H.; Horpibulsuk, S. Enhancing the Bearing Capacity of Rigid Footing Using Limited Life Kenaf Geotextile Reinforcement. *J. Nat. Fibers* **2020**, 1–17. [[CrossRef](#)]
- Abu-Farsakh, M.Y.; Chen, Q. Evaluation of geogrid base reinforcement in flexible pavement using cyclic plate load testing. *Int. J. Pavement Eng.* **2011**, *12*, 275–288. [[CrossRef](#)]
- Alimohammadi, H.; Zheng, J.; Schaefer, V.R.; Siekmeier, J.; Velasquez, R. Evaluation of geogrid reinforcement of flexible pavement performance: A review of large-scale laboratory studies. *Transp. Geotech.* **2021**, *27*, 100471. [[CrossRef](#)]

21. Ling, H.I.; Liu, Z. Performance of Geosynthetic-Reinforced Asphalt Pavements. *J. Geotech. Geoenviron. Eng.* **2001**, *127*, 177–184. [[CrossRef](#)]
22. Mirzapour Mounes, S.; Karim, M.R.; Khodaii, A.; Almasi, M.H. Improving Rutting Resistance of Pavement Structures Using Geosynthetics: An Overview. *Sci. World J.* **2014**, *2014*, 764218. [[CrossRef](#)] [[PubMed](#)]
23. Horpibulsuk, S.; Hoy, M.; Witchayaphong, P.; Rachan, R.; Arulrajah, A. Recycled asphalt pavement—Fly ash geopolymer as a sustainable stabilized pavement material. In *The IOP Conference Series: Materials Science and Engineering*; IOP Publishing: Bristol, UK, 2017.
24. Hoy, M.; Horpibulsuk, S.; Arulrajah, A.; Mohajerani, A. Strength and microstructural study of recycled asphalt pavement: Slag geopolymer as a pavement base material. *J. Mater. Civ. Eng.* **2018**, *30*, 04018177. [[CrossRef](#)]
25. Hoy, M.; Horpibulsuk, S.; Arulrajah, A. Strength development of Recycled Asphalt Pavement—Fly ash geopolymer as a road construction material. *Constr. Build. Mater.* **2016**, *117*, 209–219. [[CrossRef](#)]
26. Maghool, F.; Senanayake, M.; Arulrajah, A.; Horpibulsuk, S. Permanent Deformation and Rutting Resistance of Demolition Waste Triple Blends in Unbound Pavement Applications. *Materials* **2021**, *14*, 798. [[CrossRef](#)] [[PubMed](#)]
27. Yaowarat, T.; Horpibulsuk, S.; Arulrajah, A.; Maghool, F.; Mirzababaei, M.; Rashid, A.S.A.; Chinkulkijniwat, A. Cement stabilisation of recycled concrete aggregate modified with polyvinyl alcohol. *Int. J. Pavement Eng.* **2020**, 1–9. [[CrossRef](#)]
28. Yaowarat, T.; Horpibulsuk, S.; Arulrajah, A.; Mohammadinia, A.; Chinkulkijniwat, A. Recycled concrete aggregate modified with polyvinyl alcohol and fly ash for concrete pavement applications. *J. Mater. Civ. Eng.* **2019**, *31*, 04019103. [[CrossRef](#)]
29. Arulrajah, A.; Horpibulsuk, S.; Maghoolpilehood, F.; Samingthong, W.; Du, Y.-J.; Shen, S.-L. Evaluation of interface shear strength properties of geogrid reinforced foamed recycled glass using a large-scale direct shear testing apparatus. *Adv. Mater. Sci. Eng.* **2015**, *2015*, 235424. [[CrossRef](#)]
30. Arulrajah, A.; Kua, T.-A.; Horpibulsuk, S.; Mirzababaei, M.; Chinkulkijniwat, A. Recycled glass as a supplementary filler material in spent coffee grounds geopolymers. *Constr. Build. Mater.* **2017**, *151*, 18–27. [[CrossRef](#)]
31. Naeini, M.; Mohammadinia, A.; Arulrajah, A.; Horpibulsuk, S. Recycled Glass Blends with Recycled Concrete Aggregates in Sustainable Railway Geotechnics. *Sustainability* **2021**, *13*, 2463. [[CrossRef](#)]
32. Hoy, M.; Horpibulsuk, S.; Rachan, R.; Chinkulkijniwat, A.; Arulrajah, A. Recycled asphalt pavement—Fly ash geopolymers as a sustainable pavement base material: Strength and toxic leaching investigations. *Sci. Total Environ.* **2016**, *573*, 19–26. [[CrossRef](#)]
33. Yeheyis, M.; Hewage, K.; Alam, M.S.; Eskicioglu, C.; Sadiq, R. An overview of construction and demolition waste management in Canada: A lifecycle analysis approach to sustainability. *Clean Technol. Environ. Policy* **2013**, *15*, 81–91. [[CrossRef](#)]
34. Arulrajah, A.; Rahman, M.; Piratheepan, J.; Bo, M.; Imteaz, M. Interface shear strength testing of geogrid-reinforced construction and demolition materials. *Adv. Civ. Eng. Mater.* **2013**, *2*, 189–200. [[CrossRef](#)]
35. Suddeepong, A.; Sari, N.; Horpibulsuk, S.; Chinkulkijniwat, A.; Arulrajah, A. Interface shear behaviours between recycled concrete aggregate and geogrids for pavement applications. *Int. J. Pavement Eng.* **2020**, *21*, 228–235. [[CrossRef](#)]
36. Han, J.; Thakur, J.K. Use of geosynthetics to stabilize recycled aggregates in roadway construction. In *Proceedings of the ICSDEC 2012: Developing the Frontier of Sustainable Design Engineering, and Construction*, Fort Worth, TX, USA, 7–9 November 2012; pp. 473–480.
37. Han, J.; Thakur, J.K. Sustainable roadway construction using recycled aggregates with geosynthetics. *Sustain. Cities Soc.* **2015**, *14*, 342–350. [[CrossRef](#)]
38. Vieira, C.; Pereira, P. Interface shear properties of geosynthetics and construction and demolition waste from large-scale direct shear tests. *Geosynth. Int.* **2016**, *23*, 62–70. [[CrossRef](#)]
39. Vieira, C.S.; Pereira, P.M. Short-term tensile behaviour of three geosynthetics after exposure to Recycled Construction and Demolition materials. *Constr. Build. Mater.* **2021**, *273*, 122031. [[CrossRef](#)]
40. Suddeepong, A.; Hoy, M.; Nuntasena, C.; Horpibulsuk, S.; Kantatham, K.; Arulrajah, A. Evaluation of interface shear strength of saturated kenaf geogrid and recycled concrete aggregate for sustainable pavement applications. *J. Nat. Fibers* **2021**. [[CrossRef](#)]
41. DOH. *Standard No. DH-S 201/2544, Standard of Crusher Rock Base*; Department of Highways: Bangkok, Thailand, 2001.
42. ASTM-D6637. *Standard Test Method for Determining Tensile Properties of Geogrids by the Single or Multi-Rib Tensile Method*; ASTM International: West Conshohocken, PA, USA, 2015.
43. ASTM-D5321. *D5321M-20, Standard Test Method for Determining the Shear Strength of Soil-Geosynthetic and Geosynthetic-Geosynthetic Interfaces by Direct Shear*; ASTM International: West Conshohocken, PA, USA, 2020.
44. Disfani, M.M.; Arulrajah, A.; Bo, M.W.; Hankour, R. Recycled crushed glass in road work applications. *Waste Manag.* **2011**, *31*, 2341–2351. [[CrossRef](#)]
45. Liu, X.; Scarpas, A.; Blaauwendraad, J.; Genske, D.D. Geogrid Reinforcing of Recycled Aggregate Materials for Road Construction: Finite Element Investigation. *Transp. Res. Rec.* **1998**, *1611*, 78–85. [[CrossRef](#)]
46. Horpibulsuk, S.; Niramitkornburee, A. Pullout Resistance of Bearing Reinforcement Embedded in Sand. *Soils Found.* **2010**, *50*, 215–226. [[CrossRef](#)]
47. Sukmak, G.; Sukmak, P.; Joongklang, A.; Udomchai, A.; Horpibulsuk, S.; Arulrajah, A.; Yeanyong, C. Predicting Pullout Resistance of Bearing Reinforcement Embedded in Cohesive-Frictional Soils. *J. Mater. Civ. Eng.* **2020**, *32*, 04019379. [[CrossRef](#)]
48. Indraratna, B.; Karimullah Hussaini, S.; Vinod, J. On The Shear Behavior of Ballast-Geosynthetic Interfaces. *Geotech. Test. J.* **2012**, *35*, 305–312. [[CrossRef](#)]
49. Liu, C.-N.; Ho, Y.-H.; Huang, J.-W. Large scale direct shear tests of soil/PET-yarn geogrid interfaces. *Geotext. Geomembr.* **2009**, *27*, 19–30. [[CrossRef](#)]

50. Han, B.; Ling, J.; Shu, X.; Gong, H.; Huang, B. Laboratory investigation of particle size effects on the shear behavior of aggregate-geogrid interface. *Constr. Build. Mater.* **2018**, *158*, 1015–1025. [[CrossRef](#)]
51. Arulrajah, A.; Rahman, M.A.; Piratheepan, J.; Bo, M.W.; Imteaz, M.A. Evaluation of interface shear strength properties of geogrid-reinforced construction and demolition materials using a modified large-scale direct shear testing apparatus. *J. Mater. Civ. Eng.* **2014**, *26*, 974–982. [[CrossRef](#)]
52. Soleimanbeigi, A.; Likos, W. Mechanical Properties of Recycled Concrete Aggregate and Recycled Asphalt Pavement Reinforced with Geosynthetics. In *Geo-Congress 2019: Earth Retaining Structures and Geosynthetics*; American Society of Civil Engineers: Reston, VA, USA, 2019; pp. 284–292.
53. Pasetto, M.; Pasquini, E.; Giacomello, G.; Baliello, A. Innovative composite materials as reinforcing interlayer systems for asphalt pavements: An experimental study. *Road Mater. Pavement Des.* **2019**, *20* (Suppl. 2), S617–S631. [[CrossRef](#)]